An Efficient X-Band 16-Element Spatial Combiner of Switched-Mode Power Amplifiers

Srdjan Pajić, *Student Member, IEEE,* and Zoya B. Popović, *Fellow, IEEE*

Abstract—This paper describes the design, implementation, and characterization of a high-efficiency 10-GHz amplifier antenna array for spatial power combining. An average drain efficiency of 70% at 162 W effective isotropic radiated power, or about 1.5 W of transmitted power, is measured for an array of 16 amplifiers consisting of four four-element subarrays. The power-combining efficiency of the 16-element array is above 79%. The active device is a low-cost GaAs MESFET with a maximum available power in class A of 21 dBm. The single class-E power amplifier delivers 20.3 dBm with 67% drain efficiency and 58% power-added efficiency.

Index Terms—Active antenna arrays, high efficiency, power amplifiers (PAs), spatial power combining.

I. INTRODUCTION

SPATIAL power combining of transistor amplifiers has been a topic of research over the past decade [1]. In this approach, the powers of a large number of amplifiers are combined in free space upon radiation from an antenna array. Grid amplifiers have been demonstrated up to 35 GHz with 5-W output power at 21% efficiency [2]. Small tray arrays in waveguide have demonstrated very high power levels over the X-band of 120 W [3]. Standard antenna arrays loaded with amplifiers have also been demonstrated up to the V-band [4]–[6]. Most of these arrays are planar transmission amplifiers and, therefore, cannot have heat sinks. This results in temperature gradients across the arrays, which degrade the gain and power [7]. The problem addressed in this paper is reduction of heat dissipation and improvement of dc-power usage by increasing the power-added efficiency (PAE) and drain efficiency (η_D) of the power amplifiers (PAs). These efficiencies are maximized by operating the devices in switched mode [8] and using a low-loss corporate input network, while maintaining the spatial output power combining, as in [9]. The design of a high-efficiency active array is performed in several stages presented in the following sections.

- Section II describes the class-E PA design and characterization along with repeatability issues.
- Section III describes the antenna element design. The antenna chosen in this approach is a broad-band multilayer patch.
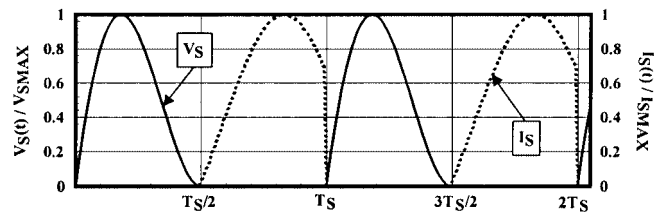
Fig. 1. Normalized transistor output voltage and current waveforms in class-E mode of operation.

- Section IV describes the four-element subarray design, including corporate feed and bias network. Measurements of the subarray are also presented and serve as a baseline for assessing the power-combining efficiency (PCE).
- Section V describes the 16-element spatial power combiner with 70% drain efficiency and 79% PCE, and the paper concludes with a summary and outlook of the applicability of this approach.

II. CLASS-E AMPLIFIER DESIGN

Class-E switched mode of operation has recently gained a lot of attention at different frequency ranges [10], [11]. Switched-mode amplifier operation was developed by Artym [12], Gruzdev [13], Popov [14], Kozyrev [15], and Sokal [16] independently for high-frequency (HF) amplifiers, and extended to microwave frequencies in a transmission-line circuit by Mader *et al.* [8], Mader and Popović [17], Bryerton *et al.* [18], and Raab *et al.* [19]. In this class of operation, the transistor is operated as a switch in such a way that the current and voltage time waveforms overlap minimally during a period. The load for this mode of operation needs to be a particular complex impedance at the design frequency, and an open circuit at all harmonics [20], resulting in theoretically 100% efficient amplification. Typical class-E transistor voltage and current waveforms normalized to the peak values for a 50% switching duty-cycle are shown in Fig. 1.

The optimal class-E load impedance [8], [17] for the transistor with the given output capacitance C_{OUT} and the operating (switching) frequency ω_S can be calculated as

$$Z_E = \frac{0.28}{C_{\text{OUT}} \cdot \omega_S} e^{j49°}. \tag{1}$$

However, since the microwave transistor has finite resistance during the ON state, and finite switching time, ideal 100% efficiency cannot be achieved. In this case, class-E waveshaping minimizes voltage and current overlapping, providing minimal losses in the active device, compared to linear classes of operation (A, AB, etc.).
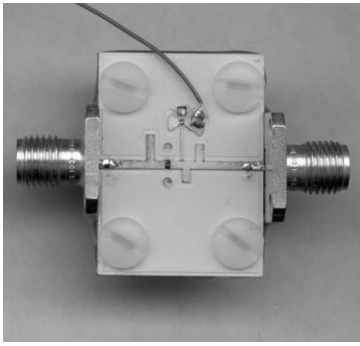
Fig. 2. Photograph of 10-GHz class-E PA used in each element of the power-combining array.

Fig. 4. Class-E PA performances over the frequency range from 9 to 11 GHz (20% bandwidth). The drain efficiency is larger than 60% over a 15% bandwidth, with a 1-dB variation in output power.

TABLE I
TYPICAL CLASS-E AMPLIFIER PERFORMANCES

P_{OUT} [dBm]	G [dB]	η_D [%]	PAE [%]	ρ [dB]
20-20.5	7-7.5	60-70	48-57	< -13

P_{OUT}: output power, G: gain, η_D: drain efficiency, PAE: power-added efficiency, and ρ: input reflection coefficient.

Fig. 5. Schematic of the broad-band patch antenna. Patches are machined on a low-cost Rogers Ultralam 2000 substrate, with $\epsilon_r = 2.43$, 0.483-mm thick. The vertical distance between patches is 2.93 mm. The feed shares the common ground plane with the directly fed patch. It is shown separated from the patch layer for clarity.
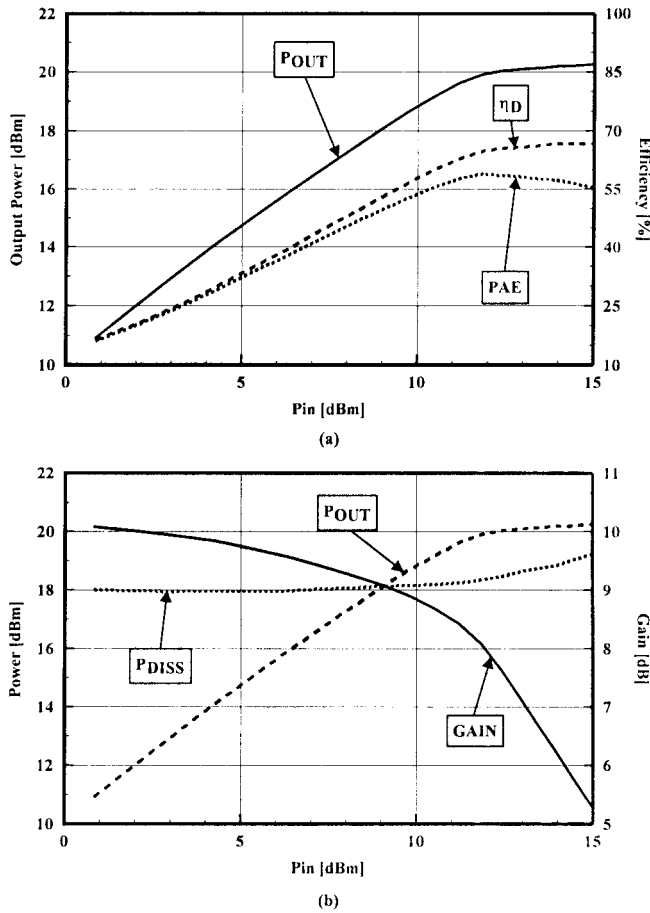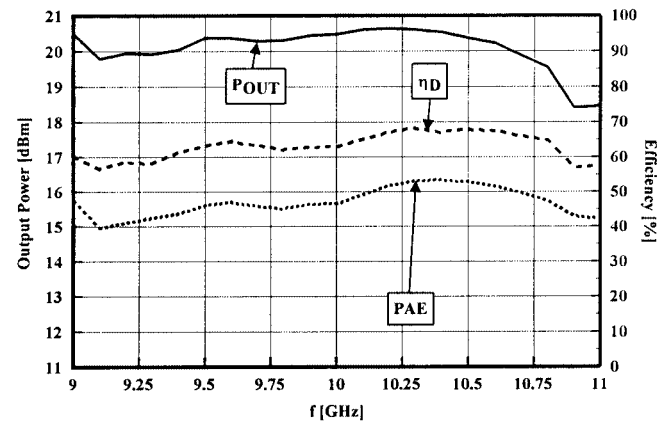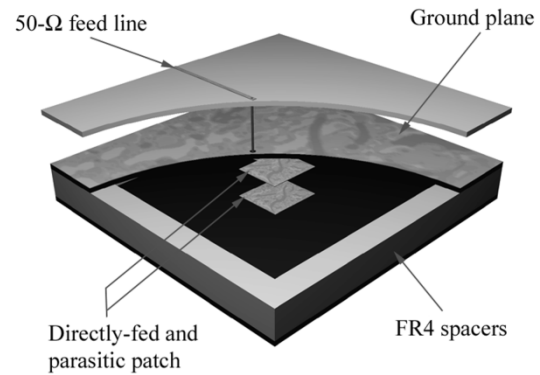

Fig. 3. Measured characteristics of the class-E PA at 10 GHz. (a) Output power and efficiency. (b) Output and dissipated power and gain as a function of input power.

For the X-band class-E PA design used in the spatial power combiner, the low-cost general-purpose GaAs MESFET AFM04P2 produced by Alpha Industries Inc., Woburn, MA, was available. The maximum drain to source voltage is 6 V and the maximum drain current is 140 mA. In class A at 18 GHz, this device is capable of delivering 21 dBm of output power with 9 dB of power gain at the 1-dB compression point. The device has useful gain up to 40 GHz. In the class-E mode of operation, voltage and current stresses on the device are higher than in linear modes of operation [17]. Taking into account the maximum device current and voltage ratings, an amplifier

designed with such a MESFET is capable of operating in sub-optimal class-E mode [21], but still with high expected drain efficiency, on the order of 60%–70%. However, due to the relatively low linear gain of the device, and the fact that it will operate deep in compression (more than 3 dB), lower PAE, on the order of 50%–60%, is expected. For an amplifier with similar performance, optical sampling measurements of time-domain voltage waveforms confirmed the approximate class-E mode of operation [22].

The first step in class-E amplifier design is the determination of the device C_{OUT}, necessary for the optimal output impedance calculation (1). If the nonlinear model of the active device is not known, manipulating given S-parameters can give a good initial estimate for the C_{OUT}. Converting S- to Y-parameters and using a simple π linear model for the device, the C_{OUT} for the selected device is found to be $C_{\text{OUT}} = 0.11$ pF. The optimal
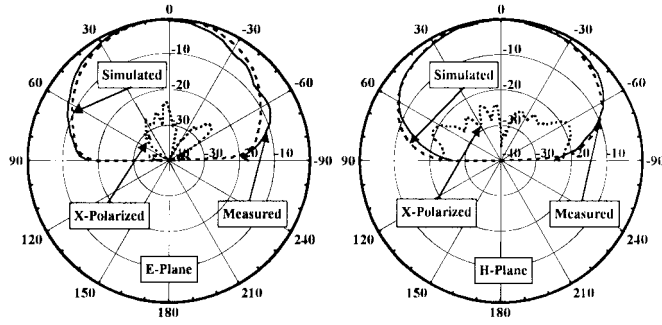
Fig. 6. Simulated and measured radiation patterns of a single stacked patch-antenna element.

Fig. 9. Measured radiation patterns of the four-element passive (dashed line) and active (solid line) antenna subarrays.
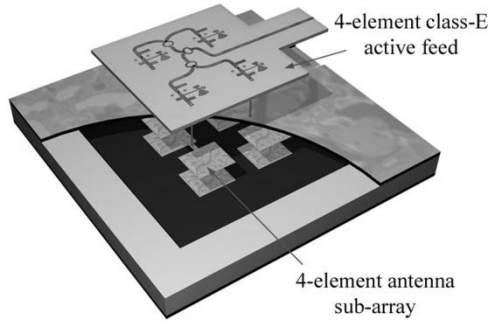

Fig. 7. Schematic of the four-element active subarray showing multiple layers. The feed layer is shown separated from the patch layer for clarity.
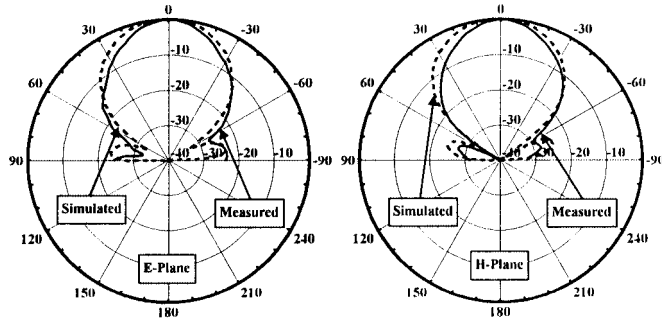

Fig. 8. Simulated (dashed line) and measured (solid line) radiation patterns of the four-element passive subarray.

Fig. 10. Power sweep characteristics of the amplifier stage in the four-element active subarray. The bounds on performance correspond to an estimated 0.5-dB uncertainty in output power measurement. The PAE shown in (b) does not include the feed loss.

class-E impedance is found to be $Z_E = (27.3 + j31.5)\ \Omega$ at 10 GHz. The input of the PA is matched starting with a conjugate match using small-signal parameters, followed by post-production tuning. This is necessary because an acceptable non-linear model for this devices does not currently exist [23]. The circuit is fabricated on a Rogers TMM6 substrate ($\epsilon_r = 6$, $h = 0.635$ mm, $t = 35\ \mu$m) (see Fig. 2).

The active device and RF decoupling capacitor are mounted on a machined copper base connected to the ground plane with conductive epoxy. The gate bias is provided through a bias tee since, in the array, it is provided through the feed. In the characterization, performing the automated bias sweep, the optimal bias point is found to be $V_{DS} = 4.2$ V, $V_{GS} = -1.4$ V, $I_{DS0} = 20$ mA. Measured output power, gain, and efficiency for the selected bias point are shown in Fig. 3.
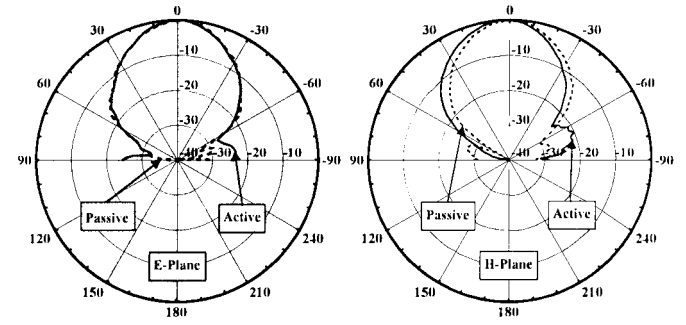
The class-E PA shows an output power flatness of 0.5 dB and drain efficiency above 60% over a 14% frequency bandwidth, as shown in Fig. 4.

In order to determine amplifier repeatability and robustness of the fabrication process, approximately 20 amplifiers were made and measured. Table I shows the range of amplifier parameters, measured at 10 GHz. Relatively narrow amplifier parameter spreading is important to achieve high PCE in the spatial combiner.
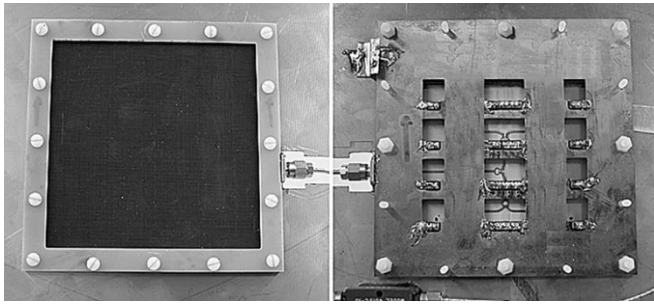
Fig. 11. Photograph of the 16-element active antenna array, front (left-hand side) and back (right-hand side). Metallized FR4 board covers the active feed, providing uniform drain bias to the active devices.
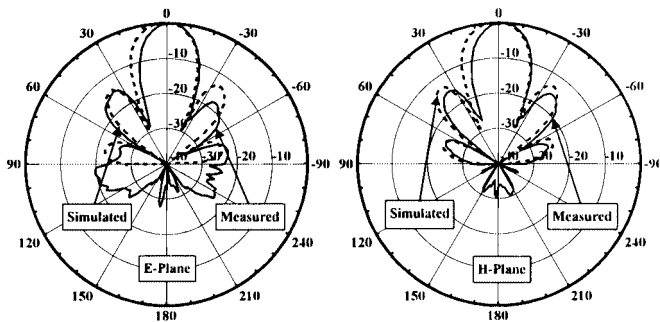
Fig. 12. Simulated and measured radiation patterns of the passive 16-element antenna array at 10.2 GHz.
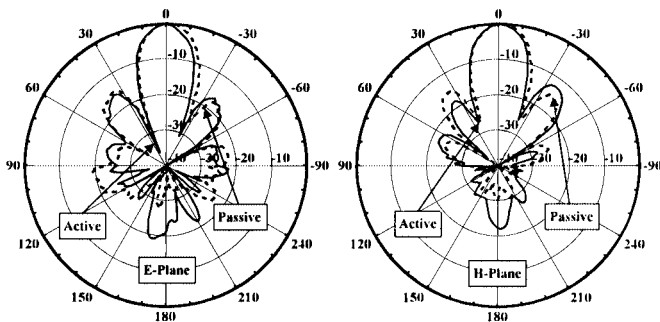
Fig. 13. Radiation patterns of the passive (dashed line) and active (solid line) 16-element antenna array at 10.2 GHz.

III. RADIATING ELEMENT DESIGN

In an active antenna element fed by a high-efficiency amplifier, variations of the optimal impedance presented to the active device can lead to performance degradation. In the case of an ordinary patch antenna, with 1%–2% frequency bandwidth, the input impedance is highly sensitive to the fabrication tolerances and material property variations. In order to provide a robust 50-Ω load to the amplifier output, a broad-band patch antenna with 2 : 1 voltage standing-wave ratio (VSWR) bandwidth of 11.6% is used. The antenna element is shown in Fig. 5.

The antenna consists of a directly fed and parasitic patch separated by an air layer. The parasitic patch is inverted and its substrate serves as a radome. Two inserted FR4 frames are used as spacers. The directly fed patch is fed by a 50-Ω microstrip line through a via-hole. The feed is fabricated on the same substrate as the amplifiers (Rogers TMM6). A common ground plane sep-
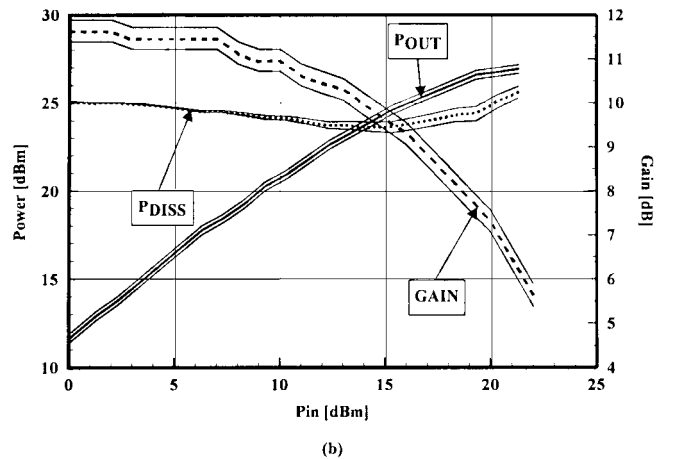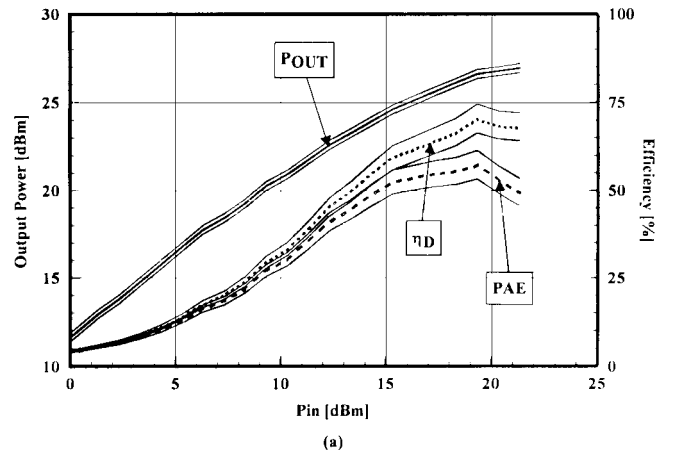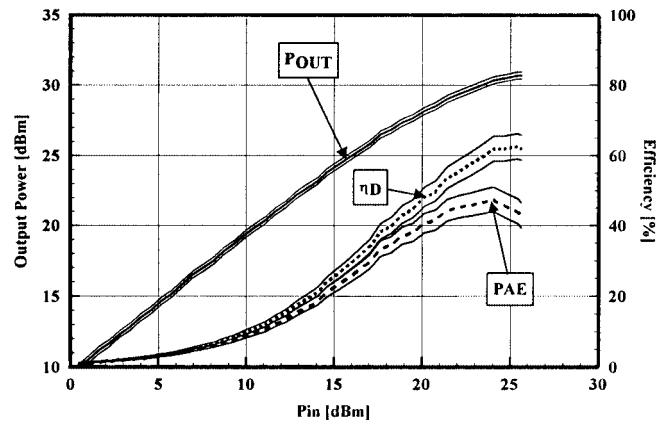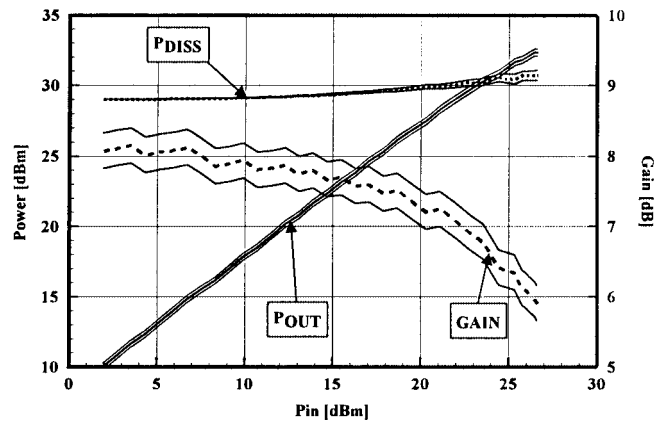

Fig. 14. Power sweep characteristics of the amplifier stage in the 16-element active array at 10.2 GHz. The bounds on performance correspond to an estimated 0.5-dB uncertainty in output power measurement.

arates the feed from the radiating side. The antenna design is optimized, using Agilent's *Momentum*. The multilayer design of the radiating-edge fed patch allows for a 50-Ω input impedance with no impedance transformer, thereby minimizing the surface area occupied by the antenna. This is required in order to have enough area for the amplifier, feeding, and biasing networks, while maintaining low mutual coupling. At 10 GHz, the antenna has an input reflection coefficient of -27 dB, with a 2 : 1 VSWR frequency bandwidth of 11.6%. The radiation pattern of the antenna element was measured in an anechoic chamber, and simulated and measured principal plane cuts are shown in Fig. 6. The simulated gain of the antenna is 8.5 dB and the measured gain, determined using the Friis formula, is 7.7 dB. The measured gain includes the feed loss.

IV. FOUR-ELEMENT ACTIVE SUBARRAY DESIGN

With the devices available for this combiner, a maximum of 1.8 W [20.3-dBm average measured PA power (see Table I)] from a 16-element combiner is expected at 10 GHz with class-E efficiency. First, a four-element subarray was designed with an antenna period of 0.6 λ_0. This period is chosen as a compromise between sidelobe levels and mutual coupling between elements that could affect the impedance presented to the amplifiers in array.
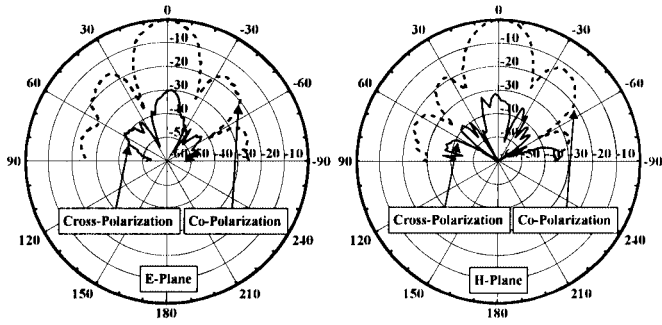
Fig. 15. Cross-polarized (solid line) patterns of the active 16-element antenna array at 10.2 GHz.
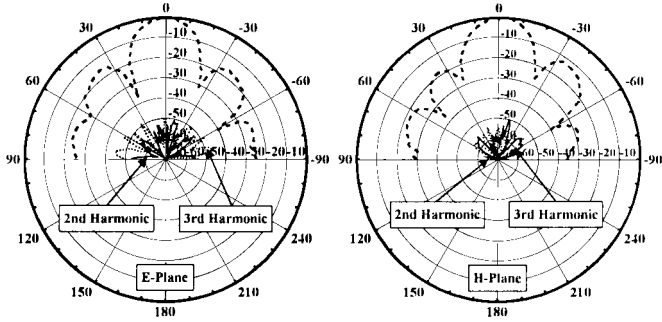

Fig. 16. Second harmonic (solid line) and third harmonic (dotted line) radiation patterns of the active 16-element array operating at 10.2 GHz.
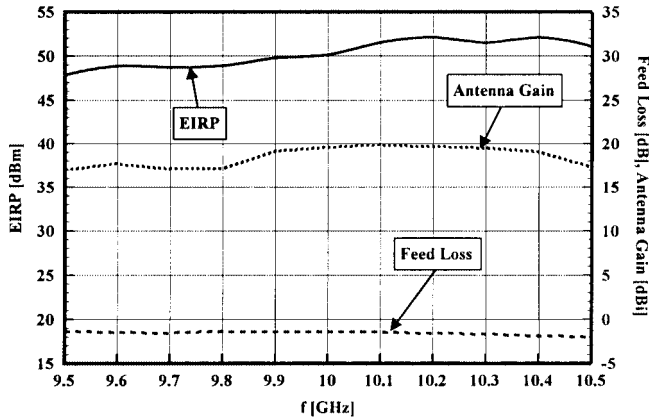

Fig. 17. Measured EIRP (solid line), feed loss (dashed line), and extracted radiation gain of the active 16-element antenna array (dotted line). Active antenna gain is calculated from the measured passive antenna gain and measured feed loss.

A corporate feed is used at the input, and a more detailed discussion on feeds for these types of power combiners is given in Section VI. The corporate feed is a one-to-four Wilkinson divider, providing good isolation between amplifiers. Based on measurements on a back-to-back divider/combiner circuit, insertion loss of the four-element feed is estimated to be 0.7 dB [24]. A schematic of the four-element subarray is shown in Fig. 7.

An additional FR4 layer (not shown in Fig. 7) connected with each amplifier bias line provides drain voltage for the active elements. This approach avoids the problem of nonuniform drain biasing addressed in [7] and eliminates potential bias-line instabilities.
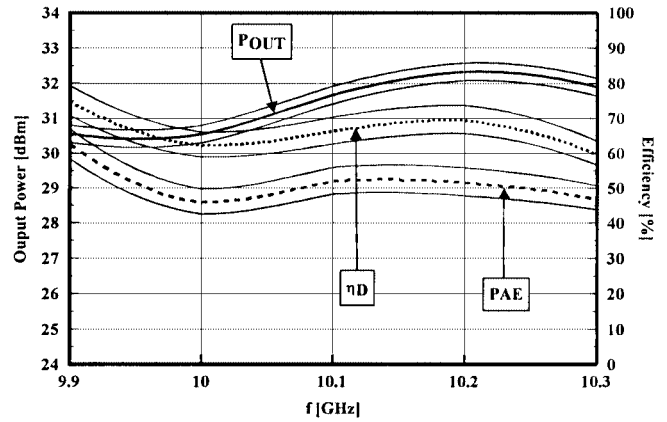

Fig. 18. Measured frequency dependence of the output power, drain efficiency, and PAE of the active 16-element array corresponding to the maximal PAE. An estimated range of values is given because directly measured output power of the amplifiers is not available.
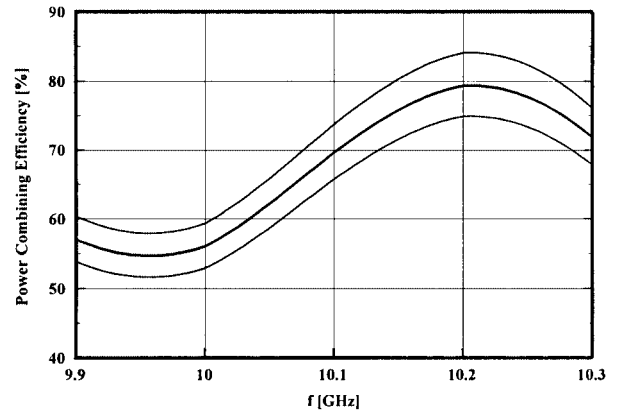
Fig. 19. Frequency dependence of the PCE for the 16-element active antenna array based on measured output power and gain.

In order to calculate amplifier efficiency, it is necessary to measure output power delivered to the radiating element. In the case of an active antenna array, this is a difficult measurement since the outputs of the amplifiers are not directly accessible. Accurate measurement of the three-dimensional (3-D) co- and cross-polarized radiation pattern, along with an estimate of antenna efficiency, can be used to calculate the output power by integration. Another approach, used in this study, is a comparative measurement. A passive antenna array, with exactly the same geometry as the active one and with the amplifiers replaced by 50-Ω thru lines, is designed and characterized in an anechoic chamber. The gain of the passive antenna, with the feed loss correction, can be found from the Friis formula for the measured input and received powers

$$G_{\mathrm{PASS}} = \left(\frac{4\pi R}{\lambda}\right)^2 \cdot \frac{P_{\mathrm{REC}}}{P_{\mathrm{IN}}} \cdot \frac{1}{G_R} \cdot \frac{1}{L_F} \qquad (2)$$

where R is the distance between the passive sub-array and receiving standard antenna with antenna gain G_R, λ is the free-space wavelength, P_{REC} is the measured power received by a standard-gain antenna, P_{IN} is the power delivered to the sub-array, and L_F is the subarray feed loss. If the passive and active antenna have the same gain, by measuring the received power

TABLE II
SUMMARIZED CHARACTERISTICS OF THE 16-ELEMENT ACTIVE ARRAY

G_{ANT} [dBi]	$EIRP$ [dBm]	η_{RAD} [%]	P_{RAD} [dBm]	PCE [%]	P_{DC} [dBm]	P_{OUT} [dBm]	η_D [%]
19.8	52.1	90	31.7	79	33.9	32.3	70

PAE [%]	P_{IN} [dBm]	ρ [dB]	P_{DISS} [dBm]	G_{AMP} [dB]	G_{ARRAY} [dB]	PAE_{ARRAY} [%]
52	28	< -13	32	5.9	3.7	34

G_{ANT}: antenna gain (feed loss excluded), EIRP: effective isotropic radiated power, η_{RAD}: simulated radiation efficiency, P_{RAD}: radiated power, P_{DC}: dc power,
P_{OUT}: amplifier output power, η_D: average drain efficiency, PAE: average power-added efficiency of the active devices, P_{IN}: input power to the array, P_{DISS}: total dissipated power in the array, G_{AMP}: gain of the entire array, and $\mathrm{PAE}_{\mathrm{ARRAY}}$: power-added efficiency of the entire array.

from the active subarray, the output power generated by the amplifiers in the array can be calculated as

$$P_{\mathrm{OUT}} = \left(\frac{4\pi R}{\lambda}\right)^2 \cdot P_{\mathrm{REC}} \cdot \frac{1}{G_R} \cdot \frac{1}{G_{\mathrm{PASS}}} \qquad (3)$$

where P_{REC} is now the measured power received by a standard-gain antenna, and G_{PASS} is the previously determined passive subarray gain. The assumption that the radiation gains of the passive and active subarrays are equal (or very similar) can be justified by comparing measured radiation patterns, with the assumption that the efficiencies of both antennas are the same. The simulated and measured radiation patterns of the four-element subarray are shown in Fig. 8.

Simulated radiation gain of the passive four-element subarray at 10 GHz is 13.2 dB, while the measured gain of the subarray is 12.8 dB. Based on a 0.7-dB estimated feed loss, the resulting gain of the passive antenna array is 13.5 dB. This value is used for active subarray output power calculations. The measured radiation patterns of the passive and active subarrays are shown in Fig. 9. The very similar radiation patterns measured for the active and passive subarrays justify using passive antenna data for estimating gain and, therefore, output power. The power sweep characteristics are shown in Fig. 10.

Since the exact values of the radiated power and radiation efficiency of the antenna are not known, a range of the measured values for the output power is given. It corresponds to a possible 0.5-dB deviation in estimated output power.

The PCE is calculated as

$$\mathrm{PCE} = \frac{P_{\mathrm{RAD}}}{N \cdot P_{\mathrm{AMP}}} \cdot 100\% \qquad (4)$$

where P_{RAD} is radiated power from the array, N is the number of array elements, and P_{AMP} is the power available from a single amplifier circuit. The PCE of the four-element subarray is 81%, with a possible error margin of $\pm5\%$.

V. 16-ELEMENT ACTIVE ARRAY DESIGN

Based on the subarray design, a 16-element active antenna array was designed with a similar 16-way Wilkinson divider as the feed and the same broad-band antenna elements. A photograph of the assembled 16-element array is given in Fig. 11. To estimate output power in the active array, a passive 16-element array was designed and simulated and measured patterns are shown in Fig. 12.

The feed loss is measured on a 16-element back-to-back Wilkinson combiner with the amplifiers replaced by 50-Ω through lines. The simulated antenna gain and radiation

efficiency of the 16-element antenna array at 10.2 GHz are 18.8 dB, and 90%, respectively, not including feed loss. When the measured feed-loss of 1.4 dB is added to the measured antenna gain (18.4 dB), a higher 19.8-dB antenna gain is obtained. It is evident from the measurement in Fig. 12 that the measured pattern is narrower than the simulated one, confirming this difference. The active antenna array radiation patterns are shown in Fig. 13 and compared to the passive array patterns. Power sweep characteristics are shown in Fig. 14.

The measured effective isotropic radiated power (EIRP) of the 16-element active array at 10.2 GHz is 52.1 dBm (162 W). As before, due to the uncertainty in determination of the antenna array gain, a range of possible values is shown, corresponding to an error in PA output power determination of ±0.25 dB. The corresponding cross-polarized radiation is shown in Fig. 15.

The second and third harmonic radiation patterns of the active array operating at 10.2 GHz are shown in Fig. 16, relative to the fundamental frequency power. Harmonic power in the signal generated by the amplifiers is significantly suppressed due to the antenna input mismatch at harmonic frequencies. The second harmonic is also suppressed by the harmonic trap in the amplifier output matching circuit, resulting in a maximal harmonic power level that is more than 45 dB below the maximum in the fundamental radiated power for both the second and third harmonics.

The measured frequency dependence of the active 16-element array EIRP, radiating gain, and feed loss are shown in Fig. 17. Based on measured EIRP and radiating gain of the active antenna, the frequency dependence of the maximal output power, corresponding drain efficiency, and PAE of the amplifier stage in the array are calculated and shown in Fig. 18. The maximum output power is measured at 10.2 GHz, and the 2% increase in optimal operating frequency is attributed to mutual coupling of elements in the array. The PCE of the 16-element active array is calculated based on a simulated radiation efficiency of the antenna array, and its frequency dependence is shown in Fig. 19. The maximum EIRP of 52.1 dBm (162 W) is observed at 10.2 GHz. At this frequency, estimated radiated power is 31.7 dBm, amplifier output power is 32.3 dBm, and the drain efficiency is 70%.

Estimation of the array parameters beyond the frequency range of 9.9–10.3 GHz becomes inaccurate due to the deviation from the initial assumption that passive and active antenna gains are equal. The average PAE is very close to the highest achieved in a microstrip amplifier. When the antenna becomes mismatched due to its limited bandwidth and mutual coupling, the amplifier performance degrades. Parameter variations
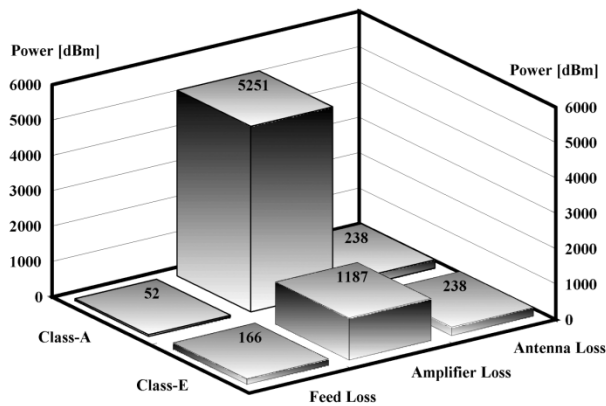
Fig. 20. Power-loss budget for the 16-element power combiner and a comparable class-A array. The antenna loss is the same for both cases. The feed loss is higher for the class-E case because the gain of the PAs is lower.

between individual amplifiers in the array (from Table I) also contribute to the degradation of the combiner characteristic. A summary of the 16-element spatial combiner at 10.2 GHz is shown in Table II.

VI. CONCLUSION

This paper describes the design, fabrication, and characterization of an X-band spatial power combiner of switched-mode PAs. The 16 active antenna elements exhibit an output EIRP of 162 W with a 70% average drain efficiency at 10.2 GHz. The PCE is estimated from measured power and gain to be above 79% at the same frequency. The four-element subarrays and the 16-element array have power-combining efficiencies around 80%, demonstrating that the array size can further be increased by arraying 16-element subarrays without significant penalty. The loss in input combining efficiency can be compensated by a driver amplifier in the feed.

The main achievement of the applied approach can be illustrated by comparison of the power-loss budgets of the designed class-E combiner with the equivalent combiner realized with the same active device operating in linear class-A mode. For this comparison, the assumed gain of the active device in class A is 11 dB and average drain efficiency is 25%. The output power is assumed to be the same as in the class-E mode. The result of a power-loss budget calculation is shown in Fig. 20. For the same output power, the dissipation in the active devices is reduced by a factor of 4.4.

In this combiner, the feed is chosen to be a corporate one since a well-known input power distribution is necessary to understand and measure the efficiency. In most other spatial combiners, the feed is spatial [5] and the argument is that feed loss remains constant for large array size. However, a spatial feed often involves nonuniform input amplitude and phase across the array. This, in turn, leads to degraded combining efficiency where the RF power is the most expensive—at the output. This problem is even more critical in a deeply saturated class-E PA, where different input power levels lead to different compression levels. This affects both output signal amplitude and phase (AM–PM conversion), significantly degrading PCE. In the combiner presented here, all PAs saturate simultaneously

as the input power is raised, and the drain efficiency across the array remains constant, maintaining the main benefit of switched-mode high-efficiency PAs.

REFERENCES

[1] R. A. York, "Quasioptical power combining," in *Active and Quasi-Optical Arrays for Solid-State Power Combining*, R. A. York and Z. B. Popović, Eds. New York: Wiley, 1997.

[2] B. Deckman, D. S. Deakin, Jr., E. Sovero, and D. Rutledge, "A 5-watt, 37-GHz monolithic grid amplifier," in *IEEE MTT-S Int. Microwave Symp. Dig.*, 2000, pp. 805–808.

[3] N. S. Cheng, P. Jia, D. B. Rensch, and R. A. York, "A 120-W X-band spatially combined solid-state amplifier," *IEEE Trans. Microwave Theory Tech.*, vol. 47, pp. 2557–2561, Dec. 1999.

[4] J. Hubert, J. Schoenburg, and Z. B. Popović, "High-power hybrid quasioptical Ka-band combiner design," in *IEEE MTT-S Int. Microwave Symp. Dig.*, vol. 2, 1995, pp. 585–588.

[5] S. Ortiz, J. Hubert, L. Mirth, E. Schlecht, and A. Mortazawi, "A high-power Ka-band quasi-optical amplifier array," *IEEE Trans. Microwave Theory Tech.*, vol. 50, pp. 487–494, Feb. 2002.

[6] J. Dixon, G. O'Dell, J. Schoenberg, S. Duncan, and Z. Popović, "60 GHz monolithic active antenna array," in *IEEE AP-S Int. Symp. Dig.*, vol. 1, 2002, pp. 38–41.

[7] T. Marshall, M. Forman, and Z. Popović, "Two Ka-band quasi-optical amplifier arrays," *IEEE Trans. Microwave Theory Tech.*, vol. 47, pp. 2568–2573, Dec. 1999.

[8] T. B. Mader, E. W. Bryerton, M. Marković, M. Forman, and Z. Popović, "Switched-mode high-efficiency microwave power amplifiers in a free-space power-combiner array," *IEEE Trans. Microwave Theory Tech.*, vol. 46, pp. 1389–1391, Oct. 1998.

[9] M. A. Gouker, J. T. Delisle, and S. M. Duffy, "A circuit-fed tile-approach configuration for millimeter-wave spatial power combining," *IEEE Trans. Microwave Theory Tech.*, pt. 1, vol. 50, pp. 17–21, Jan. 2002.

[10] J. F. Davis and D. B. Rutledge, "A low-cost class-E power amplifier with sine-wave drive," in *IEEE MTT-S Int. Microwave Symp. Dig.*, vol. 2, 1998, pp. 1113–1116.

[11] A. L. Martin and A. Mortazawi, "A class-E power amplifier based on an extended resonance technique," *IEEE Trans. Microwave Theory Tech.*, vol. 48, pp. 93–97, Jan. 2000.

[12] A. D. Artym, "Switching mode of high frequency power amplifiers" (in Russian), *Radiotekhnika*, vol. 24, pp. 58–64, June 1969.

[13] V. V. Gruzdev, "Calculation of circuit parameters of single-ended switching-mode" (in Russian), *Trudy MEI*, vol. 2, pp. 124–128, 1970.

[14] I. A. Popov, "Switching mode of single-ended transistor power amplifier" (in Russian), *Poluprovodnikovye Pribory v Tekhnike Svyazi*, vol. 5, pp. 15–35, 1970.

[15] V. B. Kozyrev, "Single-ended switching-mode tuned power amplifier with filtering circuit" (in Russian), *Poluprovodnikovye Pribory v Tekhnike Svyazi*, vol. 6, pp. 152–166, 1971.

[16] N. O. Sokal and A. D. Sokal, "Class-E—A new class of high efficiency tuned single-ended switching power amplifiers," *IEEE J. Solid-State Circuits*, vol. SSC-10, pp. 168–176, June 1975.

[17] T. B. Mader and Z. B. Popović, "The transmission-line high-efficiency class-E amplifier," *IEEE Microwave Guided Wave Lett.*, vol. 5, pp. 290–292, Sept. 1995.

[18] E. W. Bryerton, M. D. Weiss, and Z. Popović, "Efficiency of chip-level versus external power combining," *IEEE Trans. Microwave Theory Tech.*, vol. 47, pp. 1482–1485, Aug. 1999.

[19] F. H. Raab, P. Azbeck, S. Cripps, P. B. Kenington, Z. B. Popović, N. Pothecary, J. F. Sevick, and N. O. Sokal, "Power amplifiers and transmitters for RF and microwave," *IEEE Trans. Microwave Theory Tech.*, vol. 50, pp. 1527–1530, Mar. 2002.

[20] F. H. Raab, "Idealized operation of the class-E tuned power amplifier," *IEEE Trans. Circuits Syst.*, vol. CAS-24, pp. 725–735, Dec. 1977.

[21] ——, "Suboptimum operation of class-E power amplifiers," in *Proc. RF Technology Expo.*, Santa Clara, CA, Feb. 1989, pp. 85–98.

[22] M. D. Weiss, M. H. Crites, E. W. Bryerton, J. F. Whitaker, and Z. Popović, "Time-domain optical sampling of switched-mode microwave amplifier and multipliers," *IEEE Trans. Microwave Theory Tech.*, vol. 47, pp. 2599–2604, Dec. 1999.
[23] M. Marković, A. Kain, and Z. Popović, *Nonlinear Modeling of Class-E Microwave Power Amplifiers*.   New York: Wiley, 1999, pp. 93–103.
[24] S. Pajić and Z. Popović, "A 10-GHz high-efficiency active antenna sub-array," in *IEEE MTT-S Int. Microwave Symp. Dig.*, vol. 3, 2002, pp. 1527–1530.
[25] A. Grebennikov, "Class E high efficiency power amplifiers: Historical aspects and future prospects," *Appl. Microwave Wireless*, pp. 64–71, July 2002.
[26] M. D. Weiss and Z. Popović, "A 10-GHz high-efficiency active antenna," in *IEEE MTT-S Int. Microwave Symp. Dig.*, 1999, pp. 663–666.

Srdjan Pajić (S'02) received the Dipl. Ing. degree from the University of Belgrade, Belgrade, Yugoslavia, in 1995, the M.S. degree from the University of Colorado at Boulder, in 2002, and is currently working toward the Ph.D. degree in electrical engineering at the University of Colorado, Boulder.

From 1995 to 2000, he was a Research and Design Engineer with IMTEL Microwaves, Belgrade, Yugoslavia, where he was involved with the development of PAs for a radio and television broadcast system. His research interests include high-efficiency microwave PAs for active antennas, linear PAs for wireless communications, and quasi-optic power-combining techniques.

Zoya B. Popović (S'86–M'90–SM'99–F'02) received her Dipl. Ing. degree from the University of Belgrade, Serbia, Yugoslavia, in 1985, and the Ph.D. degree from the California Institute of Technology, Pasadena, in 1990.

Since 1990, she has been with the University of Colorado at Boulder, where she is currently a Full Professor. She has developed five undergraduate and graduate electromagnetics and microwave laboratory courses and coauthored (with her father) the textbook *Introductory Electromagnetics* (Upper Saddle River, NJ: Prentice-Hall, 2000) for a junior-level core course for electrical and computer engineering students. Her research interests include microwave and millimeter-wave quasi-optical techniques, high-efficiency microwave circuits, smart and multibeam antenna arrays, intelligent RF front ends, RF optical techniques, batteryless sensors, and broad-band antenna arrays for radio astronomy.

Dr. Popović was the recipient of the 1993 Microwave Prize presented by the IEEE Microwave Theory and Techniques Society (IEEE MTT-S) for the best journal paper. She was the recipient of the 1996 URSI Isaac Koga Gold Medal. In 1997, Eta Kappa Nu students chose her as a Professor of the Year. She was the recipient of a 2000 Humboldt Research Award for Senior U.S. Scientists from the German Alexander von Humboldt Stiftung. She was also the recipient of the 2001 Hewlett-Packard (HP)/American Society for Engineering Education (ASEE) Terman Award for combined teaching and research excellence.